Eye (2005) 19, 375–381

www.nature.com/eye

CLINICAL STUDY

Refractive index distribution in the porcine eye lens for 532 nm and 633 nm light

BK Pierscionek[1], A Belaidi[2] and HH Bruun[3]

Abstract

Aims **To measure the refractive index distribution in porcine eye lenses for two wavelengths from the visible spectrum: 532 and 633 nm, in order to determine whether there are any discernible wavelength dependent differences in the shape of the profile and in the magnitude of refractive index.**

Methods **Rays were traced through 17 porcine lenses of the same age group and of similar size. Ray trace parameters were used to calculate the refractive index distributions for 633 nm light in all 17 lenses and for 532 nm light in 10 lenses. The effect of the refractive index at the edge of the lens, on the rest of the profile, was considered because the mismatch between refractive index at the lens edge and the refractive index of the surrounding gel necessitated a further step in calculations.**

Results **The shape of the refractive index distributions is parabolic. There is a small wavelength dependent difference in the magnitude of the refractive index across the profile and this increases very slightly into the centre of the lens. The value of the refractive index at the edge of the lens does not appreciably affect the index profile.**

Conclusions **The wavelength dependent differences in refractive index between light of 633 and 532 nm are small but discernible.**

Eye (2005) **19,** 375–381. doi:10.1038/sj.eye.6701525
Published online 20 August 2004

Keywords: eye lens; porcine; optical properties; vision

Introduction

The optics of the eye lens varies according to species requirements and the variation is attributed to differences in lens shape and in the distribution of refractive index. The latter parameter has been the more difficult to determine chiefly because the lenticular index is not uniform. Various methods for its measurement have been tried. Studies which required slicing of the tissue[1–10] could not avoid some smearing of cellular contents across the sliced layer. More sophisticated procedures, using fibre optic sensing with minimal tissue violation, have been introduced.[11–13] Noninvasive ray tracing methods[14–22] originally derived for the measurement of refractive index distributions in optic fibre preforms[23] necessitated assumptions about the lens shape and index contours. Complex modelling techniques have also been used,[24] and more recently magnetic resonance imaging has been promoted as a method of index measurement.[25,26]

The refractive index of the lens varies with temperature and the wavelength of light but the effects of such variations on the refractive index profile have not been studied. This paper presents the first study of the refractive index distribution in the porcine lens for two different wavelengths using the method of ray tracing to see whether there is a wavelength dependent difference in the magnitude and shape of the refractive index gradient. The paper also examines the ray-tracing methods to see what effect the value of the refractive index at the lens edge has on the refractive index profile.

Materials and methods

A total of 17 porcine lenses, obtained from the local abattoir, were used in these experiments. All were used within 12 h of death. Lenses were weighed immediately after removal from the eye and reweighed after experimentation. The weight range of the lenses was 0.321–0.509 g

[1]Department of Biomedical Sciences, University of Bradford, Bradford, UK

[2]Department of Biomedical Sciences, and Department of Mechanical and Medical Engineering, University of Bradford, Bradford, UK

[3]Department of Mechanical and Medical Engineering University of Bradford Bradford, UK

Correspondence:
BK Pierscionek,
Department of Biomedical Sciences
University of Bradford
Richmond Road, Bradford
BD7 1DP, West Yorkshire
UK
Tel: +44 1274 236253
Fax: +44 1274 309742
E-mail: b.pierscionek@bradford.ac.uk

Received: 17 July 2003
Accepted in revised form: 23 February 2004
Published online: 20 August 2004

(pre-experimental weight). The difference in pre- and postexperiment weights was less than 5% in all but two lenses in which the differences were 9 and 12%. These larger differences were not the result of any alteration to the lens (eg swelling) during experimentation but due to incidents which occurred after experimentation. (In one case some of the gel medium adhered to the surface of the lens capsule; as much of this as possible was gently wiped off. In the other case, the capsule peeled off the lens on removal from the gel. Although the capsule and lens were weighed together, the sticky lens surface adhered to the spatula and some outer cell layers were lost).

During experimentation the lenses were set in a 0.5% agarose gel made up in a solvent isotonic with the aqueous, as described in previous work.[16] The lens and gel were contained in a specially designed L-shaped cell which allowed measurements to be taken in the sagittal and the equatorial planes.[16]

The optical system has been described previously.[16] Briefly, the cell containing the immobilized lens was placed in the path of parallel laser rays. The single beam source was split into 10 parallel rays in accordance with the method of Pierscionek.[27] The passage of rays through the lens was photographed using high-resolution Canon Powershot Pro70 digital camera with a total image sensor of 1 680 000 pixels. The images were transferred into a computer and analysed using the Ulead PhotoImage v.4.0 software. Ray path parameters: positions of ray entry into and exit out of the lens, and angles the emergent rays made with the optic axis were measured from the images. The maximum error in the measurement was ± 0.13 mm and $\pm 0.2^{\circ}$. Measurements were taken for the two light sources: Uniphase He–Ne class IIIb (633 nm: red) and Coherent DPSS 532 Class IIIb (532 nm: green). All lenses were subjected to ray tracing using the 633 nm source; 10 of the lenses were subjected to additional ray tracing with the 532 nm source. In all cases, measurements were made in the equatorial and the sagittal planes.

The mathematical analysis, which was applied to the measured data, was based on the method of measuring gradient index profiles in optic fibre preforms[23] as amended and described by Chan *et al*.[28] The height of the incident ray above the optic axis (y) and the angle $\psi(y)$, made by the emergent ray and the optic axis, are related to the refractive index profile $n(r)$ by the expression

$$\psi(y) = -2\cos^{-1}(y/\rho) + 2yn_s \int_{r_m}^{\rho} \frac{\mathrm{d}r}{r[r^2n^2(r) - y^2n_s^2]^{0.5}} \quad (1)$$

where: n_s is the refractive index of the surrounding medium, $n(r)$ the refractive index profile across the lens, ρ the distance of boundary from the lens centre (ie equatorial radius), and r_m the function of the displacement y and can be obtained from the equation

$$r_m n_m(r_m) = yn_s \quad (2)$$

However, when the refractive index of the surrounding medium is not matched to that of the lens edge, it is necessary to obtain an estimate of the magnitude of the refractive index mismatch before the refractive index profile can be determined.

Following Chan *et al*,[28] equation (1) can be transformed by introducing the variable ξ and a function $g(\xi)$ defined by

$$\xi = \frac{rn(r)}{n_s} \quad (3)$$

and

$$n(r) = n(\rho)\mathrm{e}^{[g(\xi)]} \quad (4)$$

to give the following expression:

$$\psi(y) = 2\{\sin^{-1}(y/\rho) - \sin^{-1}(y/\bar{n}\rho)\} - 2y \times \int_{y}^{\bar{n}\rho} \frac{\mathrm{d}\xi g'(\xi)}{(\xi^2 - y^2)^{0.5}} \quad (5)$$

where $\bar{n} = n(\rho)/n_s$ is the ratio between the refractive index at the edge of the lens ($n(\rho)$) and that of the surrounding (n_s). The term between $\{\cdots\}$ in equation (5) vanishes when the system is matched and after inversion it reduces to

$$g(\xi) = \frac{1}{\pi} \int_{\xi}^{\rho} \frac{\psi(y)\mathrm{d}y}{(y^2 - \xi^2)^{0.5}} \quad (6)$$

The effect of the refraction across the lens boundary due to index mismatch can be removed by transforming the experimentally determined refraction data $[y,\psi(y)]$ into an equivalent set of index-matched data[28] $[\bar{y}, \psi(\bar{y})]$, where

$$\bar{y} = \frac{y}{\bar{n}} \quad (7)$$

and

$$\psi(\bar{y}) = \psi(y) - 2\{\sin^{-1}(y/\rho) - \sin^{-1}(y/\bar{n}\rho)\} \quad (8)$$

The index matched data derived from equations (7) and (8) are used to calculate $g(\xi)$ (Equation (6)) which is subsequently used in Equation (4) to calculate the refractive index distribution $n(r)$.

Measurement of edge index value

The refractive index values at the extreme edge of the lens were measured by magnifying each equatorial image and applying Snell's law:

$$n_s \sin\theta_i = n_e \sin\theta_e$$

where: n_s is the refractive index of the surrounding gel, n_e is the refractive index at the lens edge, θ_i is the angle at which the ray is incident on the interface, θ_e is the angle at which the ray leaves the interface between lens surface and the surrounding medium. These measurements were taken at entry and exit points of rays in the upper or lower third of lenses. Here, refraction was sufficiently large to enable accurate measurement of refractive index at the edge of the lens to be made. Rays close to the centre did not bend sufficiently to make such calculations feasible. In all, 13 measurements were taken. The mean of these was 1.354 with a standard deviation of ± 0.002. Edge index values were only measured for 633 nm light; the 532 nm source did not provide sufficient contrast to obtain accurate values. The edge index values for 532 nm were calculated from the values measured for the 633nm source (as described in results).

Results

Refractive index profile

Figure 1 shows ray passage through the equatorial plane of a porcine lens taken for 633nm (Figure 1a) and 532 nm (Figure 1b) light. While the sagittal plane is the one relevant to the path of light in vision, the calculation of refractive index, using the Eikonal equation, requires the symmetry provided by the equatorial plane. In previous publications, the equatorial index profile was replotted for the sagittal plane by a simple transposition requiring re-scaling of the equatorial radius to the sagittal width.[16,28] The assumption underlying this transposition was that the contours of refractive index are concentric. This was supported by the findings of subsequent studies, in bovine lenses, in which the refractive index was measured directly along the optic axis[12] and the profile obtained corresponded in shape and magnitude to that found in the equatorial plane.[16,18]

The parameters necessary for the derivation of refractive index are the displacement of the incident ray from the optic axis, (y), and the angle at which each emergent ray meets the optic axis ($\psi(y)$). Figure 2(a) and (b) shows ($\psi(y)$) plotted against (y) in the equatorial plane for 633 nm and 532 nm light, respectively. Data for all lenses are combined because, in all cases, the shape in the equatorial plane is the same and the lenses were from the same age group and were of the same size. The plots were transformed into an equivalent set of index matched data (as described in the Materials and methods and using edge index values discussed below), from which the refractive index, as a function of distance from the lens centre, was calculated.

Figures 3(a) and (b) show the refractive index plotted against distance from the centre of the lens for 633 nm and 532 nm light respectively. There is a small wavelength dependent difference between the profiles and this difference increases very slightly

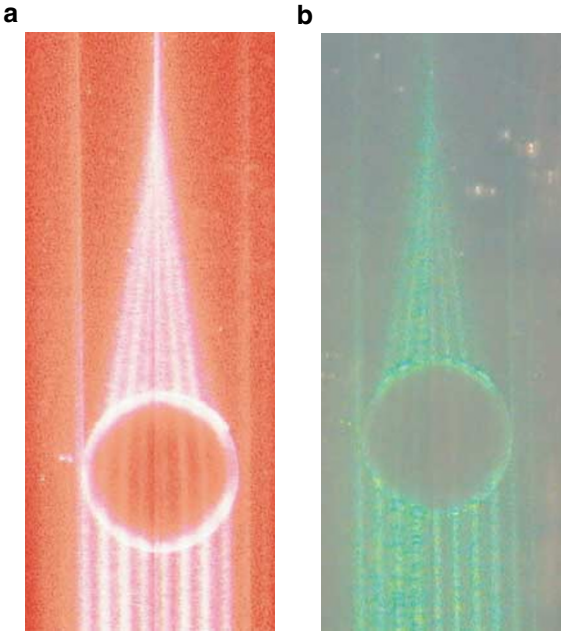

Figure 1 Ray trace photographs taken through the equatorial planes of a porcine lens for (a) 633 nm and (b) 532 nm light.

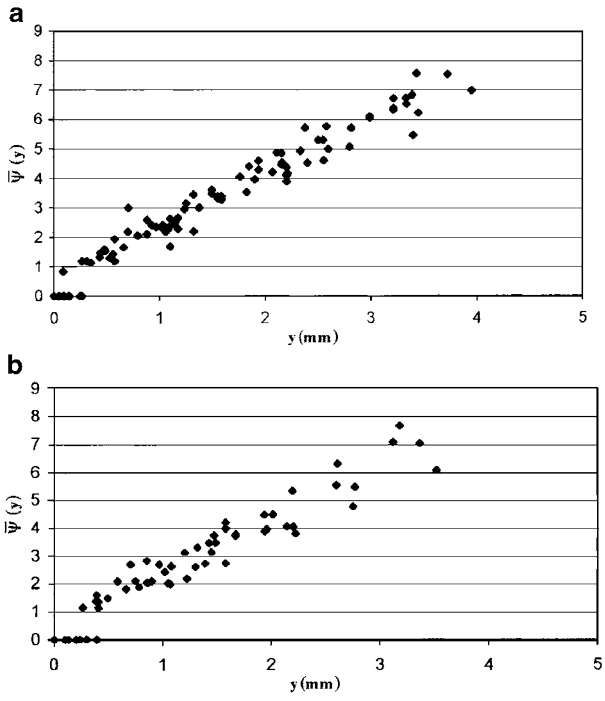

Figure 2 The angle formed by the emergent ray and the optic axis ($\psi(y)$) in degrees) plotted against the displacement of the incident ray from the optic axis (y in mm) for light of wavelength (a) 633 nm and (b) 532 nm. Measurements were made in the equatorial plane.

from periphery to centre. The index at the edge of the lens is 1.354 for 633 nm (from measurement) and 1.358 for 532 nm (from calculation described below). The index values in the central part of the lens plateau at 1.396 for 633 nm and 1.404 for 532 nm. Polynomials of second order fitted closely to both index profiles ($R^2 = 0.9760$ (633 nm); $R^2 = 0.9972$ (532 nm), $P \ll 0.005$ (both profiles)) and hence parabolic fits were considered to provide good approximations.

Edge index value

The results for 633 nm source ranged between 1.351 and 1.358, giving an average of 1.354 ± 0.002. The edge index values for the 532 nm source were more difficult to obtain because the greater scatter of the shorter wavelength light reduced the contrast of the rays. However, it was possible to calculate the index value at the edge of the lens, for 532 nm light, from protein concentrations which were obtained from the 633 nm index value by the Gladstone-Dale formula:[29]

$$n = n_s + \Delta C$$

where n is the refractive index at the edge of the lens, n_s the refractive index of the solution (in this case extracellular fluid), Δ the specific refractive increment (the increase in refractive index for every 1% increase in protein concentration (ml/g)), and C is the protein concentration (g/ml).

The refractive index of the surrounding gel was, to a close approximation, the same as water.[30] The refractive index of water at 20°C for light of 633 nm = 1.3325.[31]

Taking $n = 1.354$, $n_s = 1.333$, and $\Delta = 0.186$ ml/g (see the Appendix) gives a protein concentration at the lens edge of 0.11 g/ml. Putting this value of protein concentration back into the Gladstone–Dale formula and using $n_s = 1.337$[31] and $\Delta = 0.194$ ml/g (see the Appendix) gives an edge refractive index of 1.358 for 532 nm light.

The refractive index of the surrounding gel was not matched to the value of the index at the lens edge, requiring further calculations involving the edge index values (as described in Materials and methods). In order to see what effect the edge index value (and hence the mismatch between edge and surround indices) may have on the refractive index distribution across the lens, the edge index values for both 633 nm and 532 nm were each used with the ray trace parameters measured with 633 nm light, to calculate the respective index profiles. The distributions are shown in Figure 4 and show that the magnitude of the edge index makes little difference to the shape and magnitude of the final distribution.

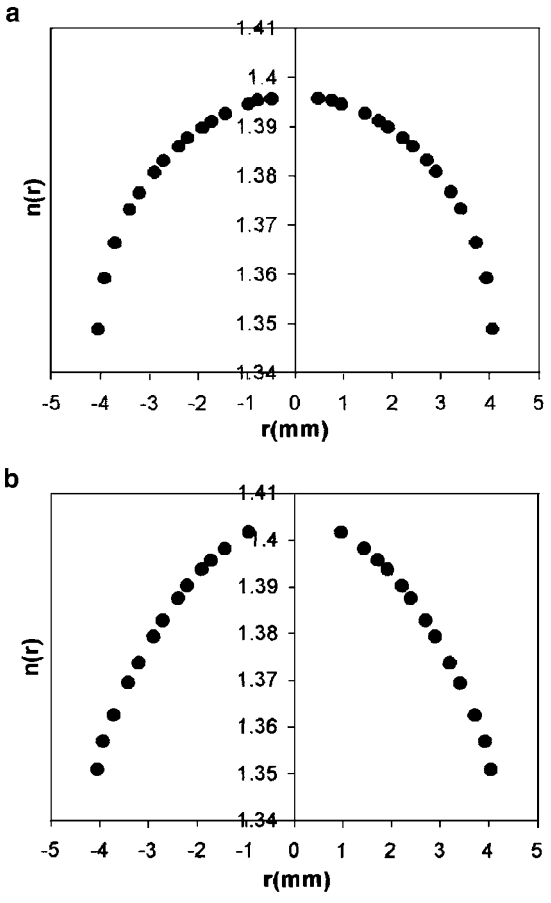

Figure 3 Refractive index ($n(r)$) plotted against radial distance from the centre of the lens (r in mm) for (a) 633 nm light and (b) 532 nm light.

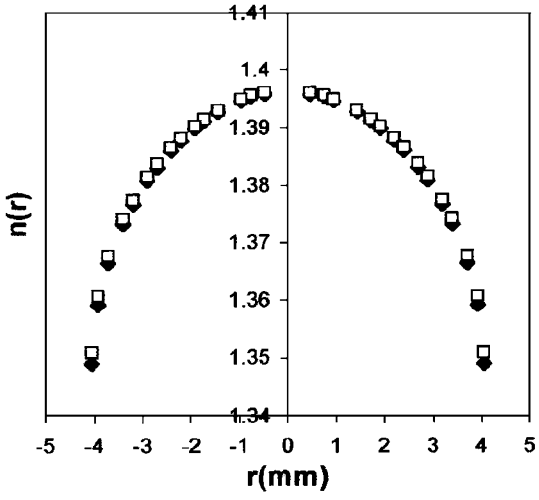

Figure 4 Refractive index ($n(r)$) plotted against radial distance from the centre of the lens (r in mm) for 633 nm using both the 633 nm (filled diamond) and the 532 nm (open square) edge index values.

Discussion

This paper, presents results of ray-trace measurements and calculations of the refractive index profiles in the equatorial planes of porcine lenses. Measurements were made for two different wavelengths, within the visible spectrum, to investigate whether any wavelength dependent variations in refractive index could be detected.

The shape of the index. profile in the porcine lens is similar to the shapes reported in other animal lenses.[7,10,12,14,16–18,21,22] The results of this study show that there is some, albeit small, wavelength dependent difference in the magnitude of refractive index: the value is slightly higher when measured with 532 nm light compared to the measurements made with 633 nm light. This is consistent with known wavelength dependent variations in refractive index: the refractive index increases as wavelength decreases. Both wavelengths were within the visible wavelength range and only about 100 nm apart and so large differences in refractive index were not expected.

Measurement of the complete refractive index gradient of the porcine lens has not been reported previously, although refractive index, for four wavelengths, has been measured, using Pulfrich refractometry, in outer and inner sections of four porcine lenses, by Sivak and Mandelman.[32] It was found that from 650 to 440 nm, the refractive index in the inner region increased from 1.4218 to 1.4346.[32] These values are higher than those reported in this study. This may be because of age differences between the lenses used by Sivak and Mandelman and the lenses used in this study. Refractive index has been shown to increase with age in bovine lenses.[18] However, as no physical dimensions were reported by Sivak and Mandelman,[32] it is not possible to make any comparisons based on age.

In terms of profile shape, the results of this study support findings from measurements of porcine lens protein concentration profiles as determined by Raman microspectroscopy.[33] This latter study showed that the profile of protein concentration in the porcine lens has a shape which could be approximated to parabolic. de Korte *et al*[33] report that the protein content rises from around 0.3 g/cm^3 in the peripheral sections of the porcine lens to around 0.7 g/cm^3 in the centre. Using these values as protein concentrations, 1.333 for the refractive index of water and 0.19 for the specific refractive increment, the Gladstone–Dale formula gives approximate refractive index values of 1.390 and 1.466 for the periphery and centre respectively. These values are higher than those found in this study and in previous work.[32] Discrepancies may be attributed to usage of different techniques and to the units of the protein content used in the presentation of results. The protein contents, reported by de Korte *et al*[33] are based on mass percentages taken as the complement of water mass, the latter calculated from the ratio of the intensities of the Raman peaks.[34] These values, therefore, give content on a relative mass/mass basis and do not take into account the partial specific volume of proteins (around 0.72 ml/g). The values derived from the Gladstone–Dale formula give concentrations as mass of solute (g) dissolved in a given volume of solvent (1 ml). Furthermore, the measurements made by de Korte *et al*[33] were made on 1 mm thick lens slices and so the result is an average value over the sample. Any method which involves slicing tissue, no matter how accurate, will cause some smearing of the contents of adjacent layers.

This study shows that there is a very small change in dispersion across the lens, increasing into the centre. This may be indicative of the variations in the proportions of the three protein classes but in the absence of data about the protein distributions in the porcine lens, no further specific conclusions can be made. Structure/function links between the proteins of the lens and the refractive index have been studied in bovine and human lenses.[35–37] No direct link between the distribution of any particular protein class and the refractive index profile has, as yet, been found. Nevertheless, some general observations, chiefly from interspecies comparisons about the structure/function relationship in the lens, are worthy of mention. The interaction between the different protein classes has an effect on water content and hence on the refractive index. Bettelheim and Finkel[38] showed that the more complex the combination of crystallin proteins, the higher the amount of water that can be absorbed. γ-crystallins (the smallest class of proteins) tend not to interact with the other protein groups and it has been noted that in species where γ-crystallin content is relatively high, for example in rat lenses, the lenses have a high protein density and therefore high refractive index. γ-crystallin is also the protein with the highest refractive increment of all the crystallins.[39] It is possible that the porcine lens has a similar pattern of protein distribution to the bovine lens, because of the similarity in shape of their respective refractive index profiles. In such case, the nuclear region of the porcine lens, should have the highest level of γ-crystallins. However, this alone cannot explain the slightly higher dispersion in the centre of the lens compared to the periphery, because the refractive increment of γ-crystallins has the lowest variation with wavelength (Appendix). The explanation is likely to lie in the structural organisation and interaction of the crystallins in the intact lens. An in depth understanding of the contribution of proteins to the optical properties will require complex models which can accurately predict and simulate the natural environment of the crystallins.

Conclusion

The complete refractive index distributions in the porcine lens have been measured for the first time for two wavelengths: 532 and 633 nm, using a ray tracing method. The two wavelengths used for the measurement were about 100 nm apart, and wavelength-related differences in the profile, were apparent. The index distributions are, like those in other animal lenses, approximately parabolic.

Acknowledgements

This work was supported by an Engineering and Physical Sciences Research Council Grant (GR/M46310).

References

1 Matthiessen L. Untersuchungen uber den aplanatismus und die periscopie der krystallsen in den augen der fische. *Pflugers Archiv* 1880; **21**: 287–307.
2 Matthiessen L. Ueber die beziehungen welche zwischen dem brechunmgsindex des kerncentrums der krystallinse und den dimensionen des auges bestehen. *Pflugers Archiv* 1882; **27**: 510–523.
3 Woinow M. Ueber die brechungscoefficienten der verschiedenen lonsenschichten. *Klin Monatsbl Augenheilkd* 1874; **12**: 407–408.
4 Freytag G. *Die breschungsindicies der linse und der flussigen augenmedien des menschen und hoderer tiere in verschiedenen lebensaltern in verleichenden unterschungen*. Wiesbaden Germany, JF Bergmann, 1908, pp 225. (Cited by Weale RA. in *The Ageing Eye* , Chapter 6: The Lens: H.K. Lewis and Co Ltd London 1963.)
5 Huggert A. On the form of the iso-indicial surfaces of the human crystalline lens. *Acta Ophthalmol (Kbh) (Suppl)* 1948; **30**: 1–126.
6 Philipson B. Distribution of protein within the normal rat lens. *Invest Ophthalmol* 1969; **8**: 258–270.
7 Nakao S, Fujimoto S, Nagata R, Iwata K. Model of refractive index distribution in the rabbit crystallin lens. *J Opt Soc Am* 1968; **58**: 1125–1130.
8 Nakao S, Ono T, Nagata R, Iwata K. Model of refractive indices in the human crystallin lens. *Jpn J Clin Ophthalmol* 1969; **23**: 903–906.
9 Palmer DA, Sivak J. Crystalline lens dispersion. *J Opt Soc Am* 1981; **71**: 780–782.
10 Jagger WS. The refractive structure and optical properties of the isolated crystalline lens of the cat. *Vis Res* 1990; **30**: 723–738.
11 Pierscionek BK. Variations in refractive index and absorbance of 670 nm light with age and cataract formation in human lenses. *Exp Eye Res* 1995a; **60**: 407–414.
12 Pierscionek BK. The refractive index along the optic axis of the bovine lens. *Eye* 1995b; **9**: 776–782.
13 Pierscionek BK. Refractive index contours in the human lens. *Exp Eye Res* 1997; **64**: 887–893.
14 Campbell MCW, Hughes A. An analytic gradient index schematic lens and eye for the rat which predicts aberrations for finite pupils. *Vis Res* 1981; **21**: 1129–1148.
15 Campbell MCW. Measurement of refractive index in an intact crystalline lens. *Vis Res* 1984; **24**: 409–415.
16 Pierscionek BK, Chan DYC, Ennis JP, Smith G, Augusteyn RC. A non-destructive method of constructing three-dimensional gradient index models for crystalline lenses: I. Theory and experiment. *Am J of Optom Physiol Optics* 1988; **65**: 481–491.
17 Axelrod D, Lerner D, Sands PJ. Refractive index within the lens of a goldfish eye determined from the paths of thin laser beams. *Vis Res* 1988; **28**: 57–65.
18 Pierscionek BK. Growth and ageing effects on the refractive index gradient in the equatorial plane of the bovine lens. *Vis Res* 1989; **29**: 1759–1766.
19 Pierscionek BK, Chan DYC. The refractive index gradient of the human lens. *Optom Vis Sci* 1989; **66**: 822–829.
20 Pierscionek BK. Presbyopia and the effect of refractive index. *Clin Exp Optom* 1990a; **73**: 26–36.
21 Jagger WS. The optics of the spherical fish lens. *Vis Res* 1992; **32**: 1271–1284.
22 Pierscionek BK, Augusteyn RC. The refractive index and protein distribution in the blue eye trevally lens. *J Am Optom Assoc* 1995; **66**: 739–743.
23 Chu PL. Nondestructive measurements of index profile of an optical fibre preform. *Elec Lett* 1977; **13**: 736–738.
24 Pomerantzeff O, Pankratov M, Wang G-J, Dufault P. Wide angle optical model of the eye. *Am J Optom Physiol Opt* 1984; **61**: 166–176.
25 Garner LF, Smith G, Yao S, Augusteyn RC. Gradient refractive index of the crystalline lens of the Black Oreo Dory (Allocyttus Niger): comparison of magnetic resonance imaging (MRI) and ray trace methods. *Vis Res* 2001; **41**: 973–979.
26 Moffat B, Atchison DA, Pope JM. Age-related changes in refractive index distribution and power of the human lens as measured by magnetic resonance micro-imaging *in vitro*. *Vis Res* 2002; **42**: 1683–1693.
27 Pierscionek BK. Method for splitting low power laser beams. *Appl Opt* 1990b; **29**: 1406.
28 Chan DYC, Ennis J, Pierscionek B, Smith G. Determination and modelling of the 3-D gradient refractive indices in crystalline lenses. *Appl Opt* 1988; **27**: 926–931.
29 Barer K, Joseph S. Refractometry of living cells. 1. Basic principles. *Q J Microsc Sci* 1954; **95**: 399–423.
30 Tucker J. The chromatic aberration of the eye between wavelengths 200 and 2000 nm: some theoretical considerations. *Br J Physiol Opt* 1974; **29**: 118–125.
31 Segelstein DJ. *The complex refractive index of water*. Thesis (MSc) Department of Physics University of Missouri-Kansas City, 1981.
32 Sivak JG, Mandelman T. Chromatic dispersion of the ocular media. *Vis Res* 1982; **22**: 997–1003.
33 de Korte CL, van der Steen AFW, Thijssen JM, Duindam JJ, Otto C, Puppels GJ. Relation between local acoustic parameters and protein distribution in human and porcine eye lenses. *Exp Eye Res* 1994; **59**: 617–627.
34 Huizinga A, Bot ACC, de Mul FFM, Vrensen GFJM, Greve J. Local variations in absolute water content of human and rabbit lenses measured by Raman microspectroscopy. *Exp Eye Res* 1989; **48**: 478–496.
35 Pierscionek BK. *The effects of development and ageing on the structure and function of the crystalline lens*. PhD dissertation, University of Melbourne, 1988.
36 Pierscionek BK, Augusteyn RC. Growth related changes to functional parameters in the bovine lens. *Biochim Biophys Acta* 1992; **1116**: 283–290.

37 Pierscionek BK, Augusteyn RC. Structure/function relationship between optics and biochemistry of the eye lens. *Lens Eye Toxicol Res* 1991; **8**: 229–243.
38 Bettelheim FA, Finkel J. Water vapour sorption of the subunits of α-crystallin and their complexes. *Colloid and Interface Science*, Vol 5. Biocolloids, polymers, monolayers, membranes and general papers New York: Acad Press Inc, 1976, pp 203–216.
39 Pierscionek BK, Smith G, Augusteyn RC. The refractive increments of bovine α, β- and γ-crystallins. *Vis Res* 1987; **27**: 1539–1541.

Appendix

The specific refractive increment varies in the third decimal place with wavelength and protein type:[39]

	546 nm	589 nm
α-Crystallin	0.195	0.190
β-Crystallin	0.189	0.187
γ-Crystallin	0.204	0.203

Data for specific refractive increments at 532 and 633 nm are not available but can be estimated assuming a linear variation in the refractive increment with wavelength. Such an estimation gives a specific refractive increment variation with wavelength as 1.16×10^{-4} for α-crystallin; 4.6×10^{-5} for β-crystallin and 2.3×10^{-5} for γ-crystallin and the following values at 532 and 633 nm:

	532 nm	633 nm
α-Crystallin	0.197	0.185
β-Crystallin	0.189	0.185
γ-Crystallin	0.204	0.202

Assuming a similar variation in protein proportions in the periphery of the porcine as of the bovine lens: α-crystallin: 50%; β-crystallin: 42%; γ-crystallin: 8%, the specific refractive increments for 532 and 633 nm are 0.194 and 0.186 ml/g, respectively.